Supporting information for:

"Grafting-Through": Growing Polymer Brushes by Supplying Monomers through the Surface

Reihaneh Mohammadi Sejoubsari,[†] Andre P. Martinez,[†] Yasemin Kutes,[‡] Zilu Wang,[§] Andrey V. Dobrynin,[§,*] and Douglas H. Adamson[†,‡,*]

[†]Department of Chemistry, and [‡]Institute of Materials Science Polymer Program, University of Connecticut, Storrs, Connecticut, USA

[§]Department of Polymer Science, University of Akron, Akron, Ohio, USA

Contents:

Details of FTIR procedure
^{1}H NMR spectra used to determine monomer concentration in kinetic studies
AFM images of dialysis bag inner surfaces
Details of computational approach used in simulations and simulation results

FTIR Details

To monitor the reactions shown in Scheme 1, FTIR was employed to identify the chemical differences between pristine, initiator functionalized, and polymer-functionalized substrates. Fourier transform infrared spectroscopy (FTIR) was performed using a Magna-IR 560 spectrometer with an ATR accessory. Samples were prepared by first drying in a vacuum oven, and were used without further modification.

Figure 5 shows, in particular, a peak centered at 1700 cm^{-1} attributed to the carbonyl absorption characteristic of the presence of the ester group expected for the initiator-functionalized substrate. Additionally, the broad band around 3300–3500 cm^{-1} implies that not all of hydroxyl groups on the surface of the membrane have reacted with initiator. The polymer-grafted dialysis bag shows a lack of the peak assigned to C=O stretching as a result of functionalization with initiator. The carbonyl stretching peak of the monomer amide groups, however, can be seen at 1650 cm^{-1}.

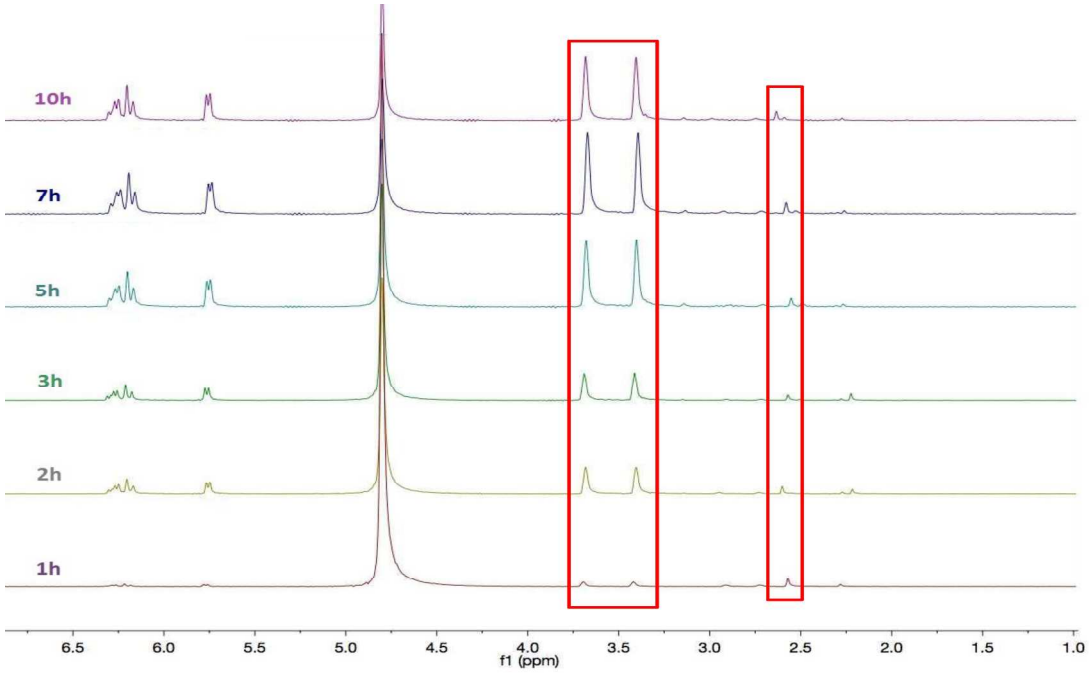

Figure S1. ^{1}H NMR spectra for the monomer concentrations coming through the Initiator-grafted dialysis bag to polymerization solution.

AFM Studies of Dialysis Bag

The reaction to functionalize the dialysis bags is carried out in THF, and the bags are observed not to swell and soften in this solvent as they do in water. The result appears to be that the functionalization reaction occurs predominately on the outer surface of the bag. The inner surface of the bag is not functionalized to a significant extent. This can be observed in Figure S2. Figure S2 A and S2 B are AFM images of inner surfaces of a dialysis bag. In Figure S2 A, the monomer is added to the outer solution so that if any initiator is present on the inner surface, the surface would appear just as we observe in Figure 2C of the main article, or Figure S2 D. In Figure S2 B, the inner surface is supplied monomer from the inside the bag, the approach used in the article. In that case, we expect the surface to appear as Figure 2B in the main article, or Figure S2 C shown for comparison. Our conclusion from these studies is that very little initiator is found on the inner surface of the dialysis bag membrane.

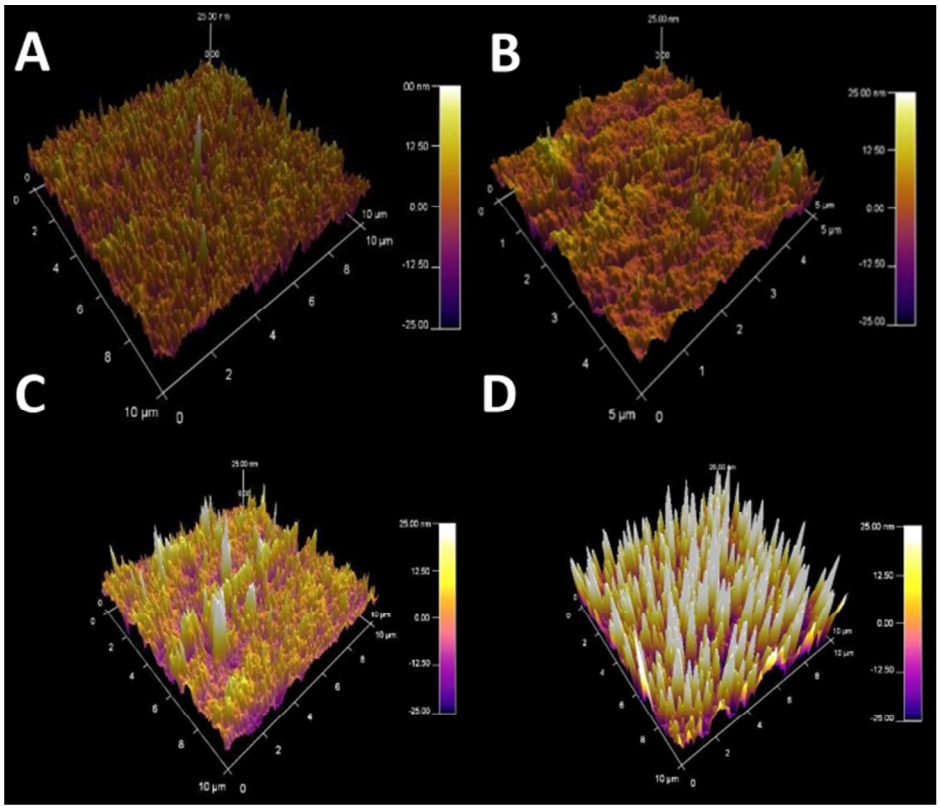

Figure S2 AFM images of functionalized dialysis bag membrane A) inner surface after bag was filled with fresh solvent and placed in a solution of monomer B) inner surface when bag was filled with monomer solution and placed in fresh solvent C) for comparison, outer surface after bag was filled with fresh solvent and placed in a monomer solution, and D) for comparison, outer surface when bag was filled with monomer solution and placed in fresh solvent.

Simulation Details

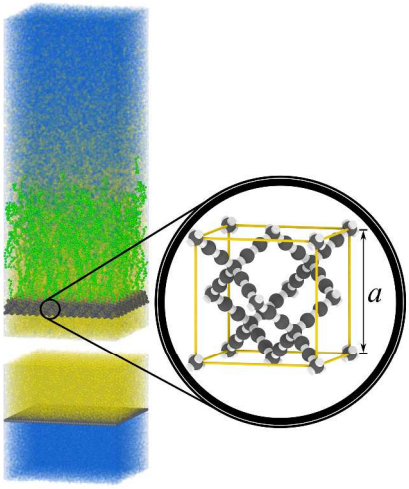

Figure S3 Snapshot of the simulation box. Brush chains are shown by green beads, catalytic sites at the chain ends are colored in yellow, monomers and solvent beads are shown by yellow and blue points respectively, piston and substrate membrane beads are shown in grey. Inset shows membrane structure.

We have performed molecular dynamics simulations[1] of the brush polymerization by a "grafting-through" approach in which monomers are supplied through a membrane. In our simulations we used a coarse-grained representation of monomers, solvent, growing polymer chains, brush supporting membrane and a piston, pushing monomers through membrane (see Figure S3).[2,3] Growing polymer chains are modeled by bead-spring chains consisting of beads with diameter σ, grafted to a substrate with grafting density ρ_g. The substrate membrane has a diamond structure with lattice parameter a = 4.44σ and a nearest inter-bead distance r_a = 0.64σ, as shown in the inset in Figure S3. The membrane had a thickness H = 4.44σ.

All beads in the system interact with WCA potential:

$$U_{WCA}(r) = \begin{cases} 4\varepsilon_{LJ}\left[\left(\frac{\sigma}{r}\right)^{12} - \left(\frac{\sigma}{r}\right)^{6}\right] + \varepsilon_{LJ} & r < 2^{\frac{1}{6}}\sigma \\ 0 & r \geq 2^{\frac{1}{6}}\sigma \end{cases} \quad \text{(S1)}$$

where the Lennard-Jones interaction parameter ε_{LJ} = 1.0 k_BT (k_B is the Boltzmann constant and T is the absolute temperature) and the cut off radius $r_{cut}=2^{1/6}\sigma$. The connectivity of beads into brush chains was maintained by the FENE bonds with:

$$U_{\text{FENE}}(r) = -\frac{1}{2}KR_0^2 \ln\left(1 - \frac{r^2}{R_0^2}\right) \quad \text{(S2)}$$

where the spring constant K = 30 k_BT and the maximum bond length R_0 = 1.5 σ . The repulsive part of the bond potential is given by the pure repulsive WCA potential with ε_{LJ} = 1.0 k_BT and r_{cut} = $2^{1/6}\sigma$ (see eq S1).

Simulations were carried out with a constant number of particles and temperature ensemble (NVT). The simulation box had dimensions 40σ x 40σ x 500σ with 3-D periodic boundary conditions. The constant temperature was maintained by coupling the system to a Langevin thermostat acting in the xy –plane only. The equation of motion of the ith bead is:

$$m\frac{d\vec{v}_i(t)}{dt} = \vec{F}_i(t) - \xi_L\vec{v}_{i_{xy}}(t) + \vec{F}_i^R(t) \quad \text{(S3)}$$

where $\vec{v}_i(t)$ is the i^{th} bead velocity, $\vec{v}_{i_{xy}}(t)$ is its projection on the xy-plane, and $\vec{F}_i(t)$ is the net deterministic force acting on the bead with mass, m, which was set to unity for all beads, and the friction coefficient ξ_L = 0.1 m/τ. $\vec{F}_i^R(t)$ is the stochastic force with zero average value $\langle\vec{F}_i^R(t)\rangle = 0$ and δ-functional

correlations $\langle \vec{F}_i^R(t)\vec{F}_i^R(t')\rangle = 4\xi_L k_B T\delta(t-t')$. The velocity-Verlet algorithm with a time step of 0.005 τ was used for the integration of equations of motion, where $\tau = \sigma(m/\varepsilon_{LJ})^{1/2}$.

To model a constant flux of monomer supply through the membrane we have implemented two different simulation schemes. In the first set of simulations the permeable membrane was moved with a constant velocity v_m = 0.01 and 0.02 σ/τ in such a way to decrease the size of the reservoir with monomers. In these simulations the location of the piston separating monomers from a solvent (see Figure S3) was kept constant. In the second set of simulations a piston separating monomers from a solvent moved with a constant velocity v_p = 0.01 and 0.02 σ/τ. In these simulations the location of the membrane was fixed. This allowed us to model the effect of the dialysis bag and provided monomer supply at a constant rate.

The catalytic sites from which brush chains being grown were attached to the membrane by rigid bonds. We have performed simulations with brush grafting densities ρ_g = $0.0625\sigma^{-2}$, $0.16\sigma^{-2}$ and $0.25\sigma^{-2}$. Each simulation was performed using the following procedure: Monomers and solvent beads were randomly distributed below and above the membrane respectively with densities $\rho = 0.729\sigma^{-3}$ (see Figure S3). To model the polymerization reaction we checked the proximity of a monomer to a catalytic site every 5 τ. If a monomer was within a cutoff radius $2^{1/6}\sigma$ from a catalytic site, we added a new monomer to a chain by creating a bond with probability 0.1. These new added monomers become a new catalytic site (active monomer).

We have also performed simulations with chain recombination in simulations when monomer flux was created by piston displacement. In these simulations, two chain ends within a cutoff radius from each other were connected by a bond and became a part of the same chain, forming a loop attached to the substrate by two ends. We checked the proximity of chain ends every 5 τ, and if the chain ends were within a cutoff radius $2^{1/6}\sigma$ from each other, we created a bond between them with probability 0.01. This allowed us to compare simulations with and without chain end recombination.

To compare brush structure obtained by "grafting through" technique with that obtained by "grafting from" method we have performed simulations of brush polymerization with monomers located above the impermeable membrane. The system parameters used in this set of simulations were identical to those used in simulations with permeable membrane.

All simulations were performed using LAMMPS.[4]

Simulation Results

The brush growth without termination is described by the ATRP reaction kinetics:

$$\frac{d\rho(t)}{dt} = -k_p[P^*]\rho(t) \qquad \text{(S4)}$$

where k_p is the rate constant, [P*] is the two dimensional number density of active propagating species (for brush growth without termination [P*] =ρ_g), and ρ(t) is the surface access of monomers, $\rho(t) =$

$\frac{N_m(t)}{L_x L_y}$, in a system at time *t*, where N_m(t) is the number of unreacted monomers in a system at time t. Integration of equation S4 results in:

$$ln\left(\frac{\rho(0)}{\rho(t)}\right) = k_p[P^*]t \quad \text{(S5)}$$

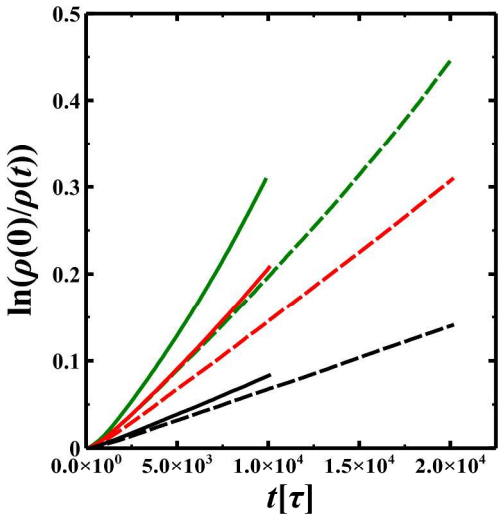

Figure S4 Evolution of monomer density during polymerization of the brush layer without chain end recombination for three different brush grafting densities: ρ_g=0.0625 σ^{-2} (black lines), 0.16 σ^{-2} (red lines) and 0.25 σ^{-2} (green lines) and two different piston velocities 0.01 σ/τ (dashed lines) and 0.02 σ/τ (solid lines).

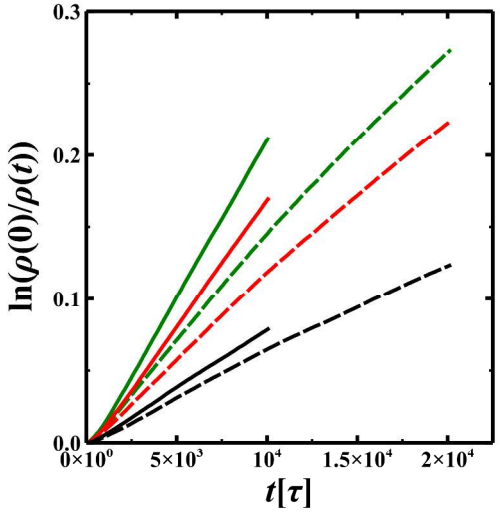

Figure S5 Evolution of monomer density during polymerization of the brush layer with chain ends recombination probability 0.01 for three different brush grafting densities: ρ_g=0.0625 σ^{-2} (black lines), 0.16 σ^{-2} (red lines) and 0.25 σ^{-2} (green lines), and two different piston velocities 0.01 σ/τ (dashed lines) and 0.02 σ/τ (solid lines).

Figure S4 verifies the expression for function $\ln(\rho(0)/\rho(t))$ during brush polymerization. For the two lowest brush grafting densities we observed almost linear growth of this function as expected from eq S5. However, for the largest grafting density this function increases faster than linear. Note that for brush polymerization with chain end recombination (see Figure S5), we see a weaker than liner increase of the function $\ln(\rho(0)/\rho(t))$ for the two larges grafting densities. This is indicative of the termination of the active centers that results from decrease the coefficient k_p in eq S5. For the lowest grafting density, the chain end recombination has almost no effect on the rate of the monomer consumption.

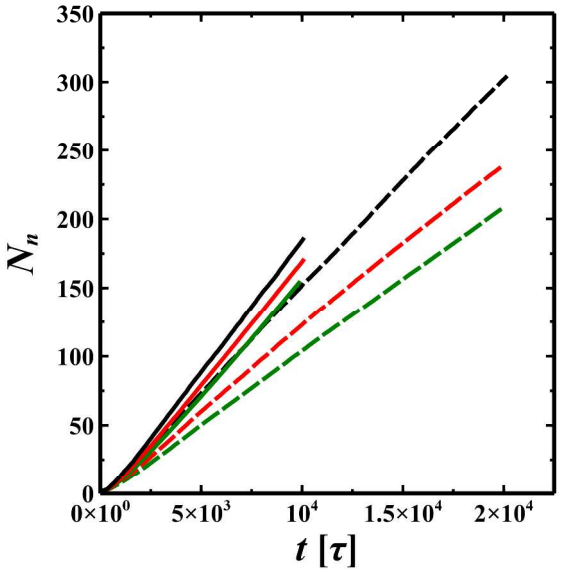

Figure S6 Dependence of the number average degree of polymerization N_n on time t for brush layers grown without end recombination. Notations are the same as in Figure S4.

In Figure S6 we plot number average degree of polymerization of brush chains, $N_n = \sum NP(N)$, obtained for different brush grafting densities and piston velocities. The number average degree of polymerization increases almost linear with time (see Figure S6).

Figure S7 shows monomer density distribution in the growing brush layer with monomers supplied by membrane (a) and piston (b) displacement with velocity 0.02 σ/τ. As one can see the evolution of the density distributions is almost identical indicating that achieved steady state is independent on how we generate monomer flux through the membrane. The concentration of the reacted monomers increases towards the edge of the brush layer while concentration of unreacted monomers decreases. There is a local depletion zone of unreacted monomer concentration at the edge of the brush layer where ends of the brush growing chains consume unreacted monomers. This reaction zone moves further away from substrate during simulation runs.

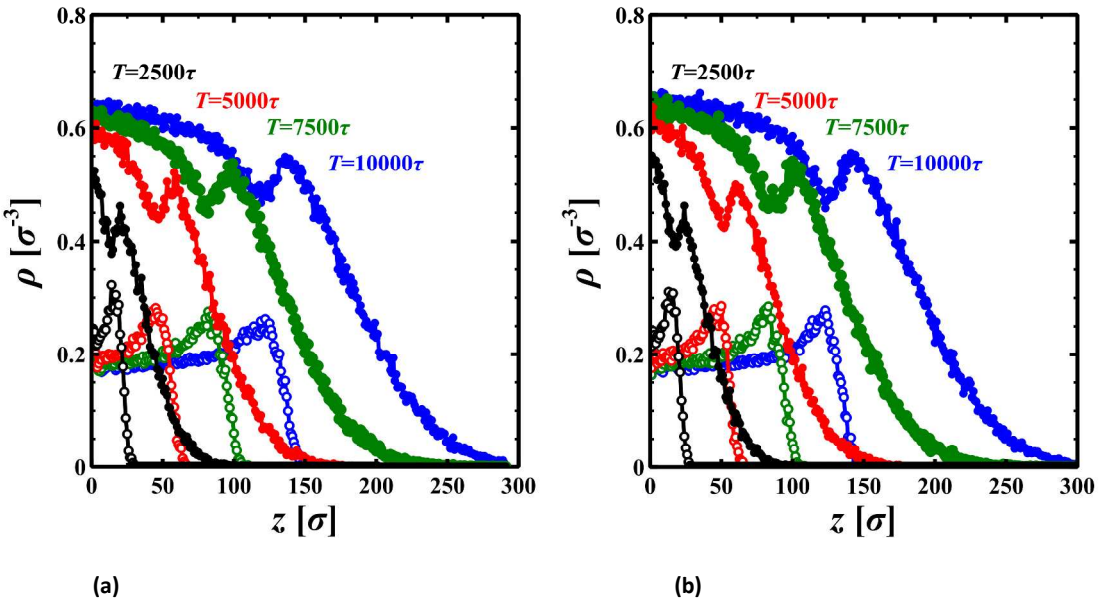

Figure S7 Density distribution of monomers in the growing brush layer without chain end recombination at time T= 2500τ (black circles), 5000τ (red circles), 7500τ (green circles) and 10000τ (blue circles) obtained in simulations with monomers supply by membrane (a) and piston (b) displacement with velocity 0.02 σ/τ and brush grafting density 0.16 σ^{-2}. Density of unreacted monomers is shown by filled symbols and the density distribution of the reacted monomers belonging to a brush is shown by open symbols.

REFERENCES

1. Frenkel, D.; Smit, B., *Understanding Molecular Simulations*. Academic Press: New York, 2002.
2. Turgman-Cohen, S.; Genzer, J. *Macromolecules* **2012,** 45, (4), 2128-2137.
3. Bain, E. D.; Turgman-Cohen, S.; Genzer, J. *Macromolecular Theory and Simulations* **2013,** 22, (1), 8-30.
4. Plimpton, S. J. *J.Comp.Phys.* **1995,** 117, 1-19.